

# **Insular cortex sub-region-dependent distribution pattern of $\alpha$ -synuclein immunoreactivity in Parkinson's disease and dementia with Lewy bodies**

Yasmine Y. Fathy<sup>1</sup>, Frank Jan de Jong<sup>2</sup>, Anne-Marie van Dam<sup>1</sup>, Annemieke J.M. Rozemuller<sup>3</sup>, Wilma D.J. van de Berg<sup>1</sup>

<sup>1</sup> Department of Anatomy and Neurosciences, section Clinical Neuroanatomy, Amsterdam Neuroscience, VU University Medical Center, De Boelelaan 1108, 1081 HZ Amsterdam, Netherlands

<sup>2</sup>Department of Neurology, Erasmus Medical Center, Rotterdam, Postbus 2040 3000 CA, Rotterdam, Netherlands

<sup>3</sup>Department of Pathology, Amsterdam Neuroscience, VU University Medical center, De Boelelaan 1117, 1081 HV Amsterdam, Netherlands

## **Corresponding author:**

Yasmine Fathy, MD

Dept. of Anatomy & Neurosciences,

Amsterdam Neuroscience

VU University Medical Center

O2 building

De Boelelaan 1108

1081 HZ Amsterdam, Netherlands

e-mail: [y.fathy@vumc.nl](mailto:y.fathy@vumc.nl); Tel.nr: +31615573540

## Abstract

The insular cortex is a heterogeneous and widely connected brain region. It plays a role in autonomic, cognitive, emotional and somatosensory functions. Its complex and unique cytoarchitecture includes a periallocortical agranular, pro-isocortical dysgranular, and isocortical granular sub-regions. In Parkinson's disease (PD), the insula shows  $\alpha$ -synuclein inclusions in advanced stages of the disease and its atrophy correlates with cognitive deficits. However, little is known regarding its regional neuropathological characteristics and vulnerability in Lewy body diseases. The aim of this study is to assess the distribution pattern of  $\alpha$ -synuclein pathology in the insular sub-regions and the selective vulnerability of its different cell types in PD and dementia with Lewy bodies (DLB). Human post-mortem insular tissues from 10 donors with incidental Lewy body disease (iLBD), PD, DLB, and age-matched controls were immunostained for  $\alpha$ -synuclein and glial fibrillary acid protein (GFAP). Results showed that a decreasing gradient of  $\alpha$ -synuclein pathology was present from agranular to granular sub-regions in iLBD, PD and PD with dementia (PDD) donors. The agranular insula was heavily inflicted, revealing various  $\alpha$ -synuclein immunoreactive morphological structures, predominantly Lewy neurites (LNs), and astroglial synucleinopathy. While dysgranular and granular sub-regions showed a decreasing gradient of inclusions and more Lewy bodies (LBs) in deeper layers. In DLB, this gradient was less pronounced and severe pathology was observed in the granular insula compared to PDD and regardless of disease stage. Protoplasmic astrocytes showed  $\alpha$ -synuclein inclusions and severe degenerative changes increasing with disease severity. While few von Economo neurons (VENs) in the fronto-insular region revealed inclusions, particularly in PDD patients. Our study reports novel findings on the differential involvement of the insular sub-regions in PD and particular involvement of the agranular sub-region, VENs and astrocytes. Thus, the differential cellular architecture of the insular sub-regions portrays the topographic variation and vulnerability to  $\alpha$ -synuclein pathology in Lewy body diseases.

**Keywords:** Lewy body pathology, insular cortex, astrocytes, von Economo neurons, selective vulnerability

# Introduction

Parkinson's disease (PD) is the second most common neurodegenerative disease, mainly characterized by motor symptoms due to the death of dopaminergic neurons in the substantia nigra pars compacta (SNpc) [24]. Yet, non-motor deficits, including cognitive impairment, autonomic dysfunction and neuropsychiatric symptoms can precede the onset of motor symptoms and are highly prevalent in PD [27, 30]. Moreover, 80% of PD patients also develop dementia (PDD) after a disease duration of approximately 10-20 years [1,50]. On the other hand, dementia with Lewy bodies (DLB), is defined by an early onset of fluctuating cognition, visual hallucinations, and dementia preceding or occurring concomitantly within one year from the onset of parkinsonism [35, 36]. PDD and DLB show considerable clinical overlap and may be considered as two ends of a disease spectrum with different timing of parkinsonism and dementia [7, 8, 44]. Despite the variation in the temporal sequence, PDD and DLB are both pathologically characterized by the presence of  $\alpha$ -synuclein aggregates in Lewy bodies (LBs) and Lewy neurites (LNs), in the brainstem, limbic and neocortical regions [12, 36]. Of interest in this respect, the insular cortex could contribute to some of the overlapping non-motor symptoms due to its wide range of functions and connections to the rest of the brain.

The insula is involved in the integration of somatosensory and autonomic information with higher cognitive functions [5, 17, 25]. It also plays a role in emotion recognition, cognition, and awareness of interoceptive information and thus acts as the basis of self-awareness [19]. It has been identified as the neural substrate for many neuropsychiatric disorders such as anxiety, depression, and bipolar disorder [28]. According to Braak staging in PD,  $\alpha$ -synuclein pathological aggregates progress from brainstem to limbic brain regions in the prodromal and early stage of the disease followed by the neocortex in more advanced stages. The insula is affected in advanced stages of the disease [12, 13]. Atrophy of the insula in PD, assessed by neuroimaging, correlated with executive dysfunction, one of the most common and early cognitive dysfunctions in PD [34]. Moreover, a reduction in dopaminergic receptor binding and grey matter density has been associated with mild cognitive impairment (MCI) in PD [18, 33]. Although the insula lately received much attention due to neuroimaging advances, little is known regarding its neuropathological characteristics in PD and DLB.

The insula is a heterogeneous region hidden deep within the Sylvian fissure and is widely connected to the brain. Macroscopically, the insula is divided into anterior and posterior gyri both constituting different cytoarchitectures. Microscopically and in order from ventro-rostral to dorso-caudal, the main sub-regions are

defined as peri-allocortical agranular (Ia), pro-isocortical dysgranular (Id), and isocortical granular (Ig) and hypergranular (G) sub-regions based on the cytoarchitecture and number of layers [23, 26, 32, 40]. According to the location and connectivity, the agranular insula relays projections mostly to limbic regions and the granular insula projects mostly to cortical areas [5, 38]. Preferential projections to the anterior insula arise from the pre-piriform olfactory, orbitofrontal, and rhinal cortices. While only the posterior insula receives projections from the 2ry somatosensory areas along with projections from cingulate cortex [38, 41]. Thus, the transition of the insular cytoarchitecture from allocortical to isocortical represents an important feature, reflecting not only its diversity but also its preferential connections and functions. Based on the current staging criteria with earlier involvement of the allocortical limbic cortex compared to the neocortex in PD, the diversity of the insular sub-regions could provide insight into the underlying characteristics predisposing to degeneration. Moreover, the presence of von Economo neurons (VENs), spindle shaped neurons in layer Vb, mostly in the agranular insula adds to the uniqueness of the region. VENs are implied to play a role in emotion, cognition, interoception, decision-making, and social awareness [4, 16].

Considering the wide-spread connectivity of the insula, the cellular heterogeneity and differential functional properties of the insular sub-regions, we hypothesize that the allocortical sub-region of the insula displays greater vulnerability than the isocortical sub-regions in PD and DLB. To gain insight in the selective vulnerability of the insular sub-regions and its cell types, we performed a detailed analysis of the  $\alpha$ -synuclein distribution pattern in postmortem brain tissues of subjects with incidental Lewy body disease (iLBD), PD and DLB.

## Materials & Methods

### Post-mortem human brain tissue

Insular post-mortem tissues from 8 donors with iLBD, PD(D), and DLB (age range: 67-93 years) and 2 age-matched controls (range: 70-78 years) were collected by the Netherlands Brain Bank and the department of Anatomy and Neurosciences, VU University Medical Center, Amsterdam. All donors had provided written informed consents for donation of brain tissue and access to clinical and neuropathological reports in compliance with ethical and legal guidelines. The main inclusion criteria were: 1) clinical diagnosis of PD(D) or DLB according to revised MDS diagnostic criteria [36, 45] and 2) pathological confirmation of diagnosis [2]. The iLBD donor had no record of neurological or neuropsychiatric symptoms yet neuropathological assessment

revealed  $\alpha$ -synuclein pathology in the brain. Subjects were excluded if they had a long history of neuropsychiatric disorders, or suffered from insular infarcts.

The entire insula was dissected into 0.5 cm thick slices and defined according to its borders with orbitofrontal and temporal cortices inferiorly and inferior frontal gyrus operculum superiorly. Tissue blocks were cryo-protected with 30% sucrose, frozen and stored at  $-30^{\circ}\text{C}$  until further processing. The tissue slices were then sectioned using a sliding microtome into 60  $\mu\text{m}$  thick sections.

### Neuropathological assessment

For neuropathological diagnosis and staging, 60  $\mu\text{m}$  paraffin sections from several brain regions of all donors were stained for  $\alpha$ -synuclein,  $\beta$ -amyloid, hyperphosphorylated tau, hematoxylin and eosin (H&E), TDP-43, and congo-red according to current consensus diagnostic guidelines [2]. Confirmation of either iLBD, PD or DLB and concomitant AD pathology was based on guidelines using Braak staging for neurofibrillary tangles (Braak NFT 0-6), Braak  $\alpha$ -synuclein (Braak  $\alpha$ -syn 0-6), Thal phase for  $\beta$ -amyloid (0-5), and ABC scoring system [10, 12, 29, 39, 51]. Glial tauopathies such as age related tauopathy of the astroglia (ARTAG) and primary age related tauopathy (PART) were assessed primarily in the temporal cortex and amygdala in all donors [20, 31].  $\alpha$ -synuclein inclusions in the insular cortex were assessed semi-quantitatively in 60  $\mu\text{m}$  sections. The semi-quantitative ordinal scoring system was developed based on the recommendations of the consensus diagnostic criteria for DLB with consideration of the tissue thickness (supplementary-Table S1).

### Immunohistochemistry

For  $\alpha$ -synuclein immunostaining, 60  $\mu\text{m}$  sections were pre-treated with 98% formic acid (Sigma, Steinheim, Germany) for 10 minutes at room temperature (RT). Endogenous peroxidase activity was blocked by 0.3%  $\text{H}_2\text{O}_2$  in Tris-buffer saline (TBS) at RT and the sections were subsequently incubated in TBS containing 0.5% Triton-x 100 (TBS-Tx), 2% bovine serum albumin, and primary antibody mouse anti- $\alpha$ -synuclein (1:2000; 610786; BD Biosciences, Europe) for 24 hours at RT. Following rinsing in TBS, the sections were incubated in the 2ry antibody biotinylated horse anti-mouse IgG (1:200, Vector) in the same buffers for 2 hours followed by standard avidin-biotin complex (1:200, Vectastatin ABC kit, Standard; Vector Laboratories, California, USA) in TBS. Then 3,3'-diaminobenzidine (DAB) was used to visualize staining. The sections were mounted and counter-stained with thionin (0.13%, Sigma) for visualization of neurons and definition of sub-regions. Adjacent sections were then immunostained with an astrocytic marker. Tissues were pre-treated with citrate buffer pH 6.0 in a steamer ( $95^{\circ}\text{C}$ ) then blocked with 5% normal donkey serum in TBS (Jackson, UK) and incubated in rabbit

anti-GFAP(1:10000; Z0334; DAKO, Denmark) in TBS-T for 72 hours at 4°C. Subsequently, sections were incubated in biotinylated goat anti-rabbit (1:200, DAKO) for 90 minutes followed by ABC (1:400) and DAB.

For immunofluorescent double staining of  $\alpha$ -synuclein and GFAP, sections were pre-treated with formic acid (98%) for 5 minutes then blocked with normal donkey serum (5%). Tissues were then incubated in rabbit anti-GFAP(1:4000; DAKO) and mouse anti  $\alpha$ -synuclein (1:1000; BD Biosciences) for 72 hours at 4 °C. This was followed by incubation in donkey anti-mouse coupled with Alexa Fluor 488 (1:400; Mol. Probes), donkey anti-rabbit coupled with Alexa Fluor 594, and Diamidino-2-Phenylindole(4,6)dihydrochloride (DAPI, Sigma) for 2 hours. The tissue sections were then mounted on glass slides and cover-slipped with mowiol as mounting medium (4-88 Calbiochem).

### Brightfield and confocal laser scanning microscopy

Digital images of the immuno-stained slides were made with a photomicroscope (Leica DM5000) equipped with color camera DFC450, Leica LASV4.4 software and 63x oil objective lens. Immunofluorescent labelling was visualized using confocal laser scanning microscopy LEICA TCS SP8 (Leica Microsystems). Image acquisition was done using 100x/1.4 NA objective lens, 405 nm diode, and pulsed white light laser (80Hz) with excitation wavelengths 405, 499 and 598nm. Deconvolution of image stacks was performed using Huygens Professional software (Scientific Volume Imaging, The Netherlands). Co-localization analyses to assess co-occurrence of GFAP and  $\alpha$ -synuclein were performed using Imaris software 8.3 (Bitplane, South Windsor, CT, USA).

### Definition of insular sub-regions

The anatomical and cytoarchitectural characteristics of the insular subregions were identified in Nissl stained sections by YF and WvdB based on the granularity and density of layers II and IV. For simplicity, definitions were based on the four known sub-regions: agranular, dysgranular, and granular/hypergranular insula [1]. The agranular insula was defined based on its ventral anterior location, absence of layers II and IV, and clusters of VENs in layer Vb. The dysgranular region is dorsal to the agranular and has more distinguished layers II and IV. The granular and hypergranular regions were defined based on their dorso-caudal and mid to posterior location and consisted of increasingly dense and granular layers II and IV [40] (Fig. 1). VENs and fork cells were assessed in layer V of the agranular insula and VENs were defined based on their spindle-shaped morphology and anatomical location [47].

# Results

## Clinical and neuropathological characteristics of PD and DLB donors

All PD(D) and DLB donors included in this study were at moderate to severe stages of disease, clinically and neuropathologically. Braak  $\alpha$ -synuclein stages ranged from III to VI and disease duration ranged from two to fifteen years. The PDD and DLB donors had moderate to severe cognitive impairments at time of death, REM sleep behavioral disorder (RBD), and several neuropsychiatric symptoms were reported including hallucinations, depression, and anxiety. During general neuropathological assessment, iLBD donor (iLBD-1) revealed  $\alpha$ -synuclein pathology in brainstem and limbic regions, according to Braak  $\alpha$ -synuclein stage IV. Moreover, ARTAG was present in PDD-1 and 2 while the latter also contained PART, both of which represent different forms of age-related tauopathy. NFT and  $\beta$ -amyloid plaques were also present in all cases, and were most severe in DLB. The demographics and neuropathological staging of all donors included in this study are summarized in Table 1.

## Distribution pattern of $\alpha$ -synuclein pathology in the insular cortex of iLBD, PD and DLB

We observed a decreasing gradient of  $\alpha$ -synuclein pathology load from the ventro-rostral agranular sub-region to the dorsal dysgranular and dorso-caudal granular sub-regions. In iLBD and PD(D),  $\alpha$ -synuclein deposits were present in all grey matter layers of the agranular insula, whereas in the dorsal dysgranular less immunoreactivity was observed. The  $\alpha$ -synuclein immunoreactivity was minimal or absent in the granular insula. LNs were present in all layers while LBs were predominantly found in the deep layers V and VI. In DLB cases, the gradient was less pronounced due to the presence of severe inclusions in all sub-regions and an abundance of LBs in layer V-VI with relative sparing of layer III/IV in the granular insula (Supplementary Table S1).

The iLBD insular cortex (iLBD-1), assessed at the level of mid-insula, showed few LN in both agranular and dysgranular regions and very mild immunoreactivity in the granular insula (Table S1).  $\alpha$ -synuclein immunoreactive features consisted of dot-like deposits, few LNs, sparse LBs, and some astroglial deposits (Fig. 2 a-c). PD-1 revealed very sparse  $\alpha$ -synuclein inclusions in all sub-regions, more pronounced in the agranular insula and mild inclusions in the white matter of granular insula (Fig. 2 d-f). PD-2 showed moderate to severe LN and few LBs in the deep layers of the agranular insula. The granular and dysgranular sub-regions contained bulgy LNs as well as a mild to moderate number of LNs and LBs, respectively (Fig. 2 g-i).

In PDD 1-3, the same gradient of  $\alpha$ -synuclein immunoreactivity was present with highest load of pathology in agranular insula. PDD-1 showed very long LNs in the superficial layers of the agranular insula and a mild to

moderate  $\alpha$ -synuclein load in the granular and dysgranular insula, respectively. Astroglial  $\alpha$ -synuclein inclusions were also found in PDD 1 and 2 (Fig. 2 j-o). In contrast, DLB-1 and 2 showed severe  $\alpha$ -synuclein inclusions in all layers and sub-regions and severe protoplasmic astroglial  $\alpha$ -synuclein inclusions (Fig. 2 p-u).

### **Morphology of $\alpha$ -synuclein immunoreactive structures in the insular cortex**

In PDD cases with astroglial tauopathy (PDD 1 and 2), severe synucleinopathy was observed in astrocytes (Fig. 3 a-b). The supragranular layers I-III, showed moderate to severe LNs variable in shape and size, thread-like, bulgy and long. Layers V and VI contained LNs and predominance of cortical LBs, increasing in gradient from agranular to granular sub-regions. DLB insular tissues also showed astroglial  $\alpha$ -synuclein deposits, severe load of LNs, and cortical LBs throughout multiple layers but predominantly in layers V and VI (Fig. 3-c). Astrocytes with multiple varicosities were predominantly found in the agranular and to a lesser extent in the dysgranular insula, in both controls and patients, possibly representing varicose projection astrocytes. And in PDD and DLB, degenerative changes in the form of detached astroglial processes with bulbous and doughnut-shaped end-feet were present in superficial layers. Some degenerated astrocytes in grey and white matter also contained granular accumulations along their processes, possibly representing fuzzy astrocytes (Fig. 3 d-f).

### **Neuronal vulnerability in insular cortex**

Only 1-2% of VENs and few fork cells in layer V of fronto-insular region revealed  $\alpha$ -synuclein inclusions in PD-2 and PDD 1 and 2. VENs showed granular cytoplasmic  $\alpha$ -synuclein inclusions and Lewy bodies. They were also frequently surrounded by astroglial cells showing thorn-shaped  $\alpha$ -synuclein immunoreactivity. In DLB, VENs were surrounded by inclusions but the precise location of these inclusions, intracellular or extracellular, could not be discerned due to the severe extent of pathology within the agranular sub-region (Fig. 4).

### **Relationship between astrocytes and $\alpha$ -synuclein pathology**

Double labelling of GFAP and  $\alpha$ -synuclein was performed to examine the relationship between astrocytes and  $\alpha$ -synuclein inclusions. A varicose projection astrocyte (VPA) in the infragranular layer in PD-2 was found containing a cluster of cytoplasmic  $\alpha$ -synuclein forming a mesh-like structure (Fig. 5-a). Further colocalization analysis in all cases assessing the co-occurrence and correlation of  $\alpha$ -synuclein and GFAP in VPA showed an inverse correlation, using Pearson's correlation coefficient (PCC), in colocalized volume (PCC: -0.09). While Mander's overlap coefficient (MOC) showed a large correlation between  $\alpha$ -synuclein and GFAP (MOC= 0.93

and 0.27). The 3D reconstruction indicated possible compartmentalization of the  $\alpha$ -synuclein within the astrocytic cell body (Fig. S1). Other protoplasmic and interlaminar astrocytes examined in PDD and DLB showed  $\alpha$ -synuclein deposits around the cell body and processes (Fig. 5-e) and a large correlation between GFAP and  $\alpha$ -synuclein was observed using MOC (Fig. S1).

## Discussion

In this case series, we observed a decreasing gradient in the load of  $\alpha$ -synuclein immunoreactivity from the anterior periallocortical agranular sub-region to the intermediate pro-isocortical dysgranular, and posterior isocortical granular insula of iLBD, PD and DLB subjects. This was particularly evident in iLBD and PD(D) with highest load of neuropathological inclusions in the agranular insula. In DLB, there was also extensive  $\alpha$ -synuclein immunoreactivity in the granular region with an abundance of LBs in the infragranular layers V/VI, glial inclusions, and relative sparing of layers III/IV. Some VENs in the anterior insula revealed  $\alpha$ -synuclein inclusions in PD(D). Astrocytes were also vulnerable to  $\alpha$ -synuclein inclusions and showed degenerative changes at all disease stages yet most prominent in PDD and DLB. The agranular and to a lesser extent, dysgranular insula in all donors revealed varicose projection astrocytes.

The presence of a gradient across the insula from the agranular to more granular sub-regions has been previously documented for NFT and  $\beta$ -amyloid pathology in AD [9]. This decreasing pathological gradient appears to be consistent with differences in terms of cytoarchitecture, cell types, and myelination in the insula. Accordingly, the agranular insula comprises the highest density of acetylcholinesterase and lowest density of myelinated fibers while the opposite exists in the granular sub-regions [37]. The vulnerability of the agranular insula relative to the late and sparse involvement of the granular corresponds with an inverse relationship between myelination and neuropathological lesions in both AD and PD [14]. The agranular insula also comprises of preferential connections to the olfactory and rhinal cortices which are affected in early stage PD and show a similar allocortical cytoarchitecture [13, 38]. In line with this, the granular insula connects to isocortical somatosensory and cingulate cortex and is affected in later stages of the disease [38]. Thus the cytoarchitecture and the connectivity of the insular subregions could provide a framework for the understanding of dissemination of  $\alpha$ -synuclein pathology throughout the brain [11, 21]. Considering the anterior insula connectivity,  $\alpha$ -synuclein pathology and cell death in the agranular insula may also contribute to autonomic, cognitive and psychiatric symptoms in PD(D) and DLB [52].

According to the Braak staging criteria for PD, the progression of  $\alpha$ -synuclein pathology follows a predictable pattern. Initially,  $\alpha$ -synuclein inclusions start in the brainstem and spread caudally in the mesencephalon in stages I-III, to the mesocortex in stage IV while increasing in density and spreading to the neocortex in stages V and VI [12]. Considering the insular phylogenetic and ontogenetic variations [6], the insular sub-regions alone could reflect the global regional involvement in PD as described by Braak and colleagues. For instance, the agranular insula was shown to contain neuropathological inclusions from stage III which increased with advanced stages. While the granular insula showed mostly absent to mild inclusions at stages III & IV, and a mild to moderate load of LNs and LBs in the deep layers in stages V & VI in PDD. Yet, the pathological assessment of the insula in PD is not routinely included in all scoring criteria and is not assessed on a sub-regional basis [3]. Taking into account its allocortical to isocortical transition, assessment of the insular sub-regions could provide us with insight into disease progression in PD and DLB.

Furthermore, in our study, the granular insula in DLB showed a greater load of  $\alpha$ -synuclein deposits compared to PDD and regardless of disease stage. Despite the greater vulnerability of the granular insula to  $\alpha$ -synuclein deposits, relative sparing of layers III/IV was observed. The reduced vulnerability of these layers could be related to their further development in granular insula compared to other sub-regions, with an increasing number of neurons, parvalbumin-positive interneurons, and myelinated fibers [40]. Along with a shorter disease duration and early onset of cognitive/ neuropsychiatric deficits, DLB brains showed higher NFT and  $\beta$ -amyloid staging along with an extensively greater load of  $\alpha$ -synuclein pathology in all regions including granular insula. We therefore highlight the higher vulnerability of neocortical regions, as represented by the granular insula, in DLB compared to PDD. This is important as both DLB and PDD overlap clinically and neuropathologically with an earlier onset of dementia in DLB.

We also show that VENs are vulnerable to  $\alpha$ -synuclein pathology in advanced PD(D). VENs have been implicated in consciousness, interoception, emotion, cognition, and social awareness [4, 22, 47]. In this study, about 1-2% of VENs showed  $\alpha$ -synuclein inclusions compared to the greater involvement of pyramidal neurons within the agranular insula. Previous studies assessing VENs found tau inclusions as well as significant cell loss in Pick's disease compared to AD [46]. VENs are projection neurons with a uniquely and sparsely branched basal dendrites. They are known to be selectively vulnerable to degeneration early in frontotemporal dementia as well as early onset schizophrenia [26]. Despite previous implications on the possible role of VENs in PD, our study is the first to show their involvement in PDD and DLB. The VENs unique properties, location, and

functions could help elucidate their role in the development of cognitive and neuropsychiatric deficits in PDD and DLB.

Astrocytes have been previously shown to contain  $\alpha$ -synuclein inclusions in advanced PD and parallel to the neuronal involvement [15]. However, minimal astrocytic activation and cytoplasmic  $\alpha$ -synuclein inclusions were observed in PD compared to other neurodegenerative diseases [49]. In our series, we observed the enwrapment of astrocytic cell bodies and processes with  $\alpha$ -synuclein. Protoplasmic and interlaminar astrocytes showed extensive synucleinopathy most severe in the agranular insula, particularly in PDD with glial tauopathy and DLB. Astroglial tauopathy could play an important role by functioning as a potential seed for glial synucleinopathy and leading to further degeneration by promoting their oligomerization and coaggregation [48]. Yet another unique feature in the agranular insula, was the presence of varicose projection astrocytes (VPA). These recently discovered astrocytes with varicosities along their processes were found only in higher order primates and humans [43]. Recent studies proposed that they may provide alternative pathways for long distance communication through cortical layers [42, 43]. We report a selective topographic distribution of these cells with predominance in agranular insula and development of intracellular inclusions in PD.

The limitations of this study include a small sample size, limited range of neuropathological stages and lack of longitudinal clinical data on the cognitive and psychiatric performance of the included PD and DLB patients. Future studies including a large number of cases and quantitative assessment of related proteinopathies could warrant a better understanding of the selective vulnerability of different cell types and their connections in the insular sub-regions in neurodegenerative diseases. Moreover, assessment of the relationship between insular pathology, cognitive phenotypes and psychiatric disturbances in PD and DLB could also provide further clues towards the substrates of cognitive and neuropsychiatric deficits in these disorders.

## Conclusions

In conclusion, the distribution pattern of  $\alpha$ -synuclein pathology revealed a decreasing anterior-to-posterior gradient in the insular cortex representative of the differential cytoarchitectural vulnerability in PD.  $\alpha$ -synuclein pathology was more pronounced in the posterior isocortical insula in DLB compared to PDD and regardless of disease stage, thus portraying differences between these two entities. Yet, DLB and PDD cases that presented with astroglial tauopathy shared a similar astrocytic involvement and extensive astroglial synucleinopathy. We also show, for the first time, the vulnerability of VENs to  $\alpha$ -synuclein pathology which may in turn contribute to cognitive and neuropsychiatric deficits in these diseases. Considering the widespread insular connectivity and

functions, we propose future considerations of the insular subregions for neuropathological assessment and for differential postmortem diagnosis of PD(D) and DLB.

### Abbreviations

AD: Alzheimer's disease ARTAG: Age related tauopathy of the astroglia DLB: Dementia with Lewy bodies, GFAP: glial fibrillary acidic protein iLBD: incidental Lewy body disease LB: Lewy bodies LN: Lewy neurites MOC: Mander's overlap coefficient NFT: Neurofibrillary tangles PART: primary age related tauopathy PCC: Pearson's correlation coefficient PD: Parkinson's disease PDD: Parkinson's disease with dementia RBD: REM sleep behavioral disorder VENS: von Economo neurons VPA: varicose projection astrocytes

### Acknowledgments

This work was funded by Stichting ParkinsonFonds, the Netherlands.

The authors are thankful to all donors and their families for making this research possible. We would like to express our gratitude for the efforts of the Netherlands Brain Bank team for providing the necessary material and data. Finally, we would like to thank Evelien T. Huisman, Lucienne te-Bulte Baks, Allert J. Jonker, and John Bol for technical assistance.

### Funding

This study was funded by Stichting ParkinsonFonds, The Netherlands

### Declarations

The authors declare having no competing interests.

### Author Contributions

The study design was carried out by WB and YF. YF carried out the experimental work and wrote the initial manuscript. WB and AR performed the autopsies and the diagnostic scoring. AD provided technical advice and revised the manuscript. FJ participated in the design and revised the manuscript. Significant contributions were provided by WB, AD, AR, and FJ and the manuscript was then edited and finalized by YF and WB.

## Bibliography

- [1] Aarsland D, Andersen K, Larsen JP, Lolk A, Nielsen H, Kragh-Sørensen P (2001) Risk of dementia in Parkinson's disease: a community-based, prospective study. *Neurology* 56: 730-6.
- [2] Alafuzoff I, Ince PG, Arzberger T, Al-Sarraj S, Bell J, Bodi I, et al (2009) Staging/typing of Lewy body related alpha-synuclein pathology: a study of the BrainNet Europe Consortium. *Acta Neuropathol.* 117: 635-52.
- [3] Alafuzoff I, Parkkinen L. (2014) Staged pathology in Parkinson's disease. *Parkinsonism Relat Disord.* 20: S57-61 .
- [4] Allman JM, Tetreault NA, Hakeem AY, Manaye KF, Semendeferi K, Erwin JM, Park S,

- Goubert V, Hof PR (2010) The von Economo neurons in fronto-insular and anterior cingulate cortex in great apes and humans. *Brain Struct Funct.* 214: 495-517.
- [5] Augustine, JR (1996) Circuitry and functional aspects of the insular lobe in primates including humans. *Brain Research Reviews* 22: 229–244.
- [6] Bauernfeind AL, de Sousa AA, Avasthi T, Dobson SD, Raghanti MA, Lewandowski AH, Zilles K, Semendeferi K, Allman JM, Craig AD, Hof PR, Sherwood CC (2013) A volumetric comparison of the insular cortex and its subregions in primates. *J Hum Evol.* 64: 263–279.
- [7] Berg D, Postuma RB, Bloem B, Chan P, Dubois B, Gasser T, et al (2014) Time to redefine PD? Introductory statement of the MDS Task Force on the definition of Parkinson's disease. *Mov Disord.* 29: 454-62. doi: 10.1002/mds.25844.
- [8] Boeve BF, Dickson DW, Duda JE, Ferman TJ, Galasko DR, Galvin JE, et al (2016) Arguing against the proposed definition changes of PD. *Mov Disord.* 31: 1619-1622.
- [9] Bonthius DJ, Solodkin A, Van Hoesen GW (2005) Pathology of the insular cortex in Alzheimer disease depends on cortical architecture. *J Neuropathol Exp Neurol.* 64: 910-22.
- [10] Braak H, Alafuzoff I, Arzberger T, Kretschmar H, Del Tredici K (2006) Staging of Alzheimer disease-associated neurofibrillary pathology using paraffin sections and immunocytochemistry. *Acta Neuropathol.* 112: 389-404.
- [11] Braak H, Del Tredici K (2016) Potential Pathways of Abnormal Tau and  $\alpha$ -Synuclein Dissemination in Sporadic Alzheimer's and Parkinson's Diseases. *Cold Spring Harb Perspect Biol.* 8:: a023630. doi: 10.1101/cshperspect.a023630
- [12] Braak H, Del Tredici K, Rüb U, de Vos RA, Jansen Steur EN, Braak E (2003) Staging of brain pathology related to sporadic Parkinson's disease. *Neurobiol Aging* 24: 197-211.
- [13] Braak H and Del Tredici K (2009) *Neuroanatomy and Pathology of Sporadic Parkinson's Disease.* Springer, Berlin.
- [14] Braak H, Rüb U, Schultz C, Del Tredici K (2006) Vulnerability of cortical neurons to Alzheimer's and Parkinson's diseases. *J Alzheimers Dis.* 9: 35-44.
- [15] Braak H, Sastre M, Del Tredici K (2007) Development of alpha-synuclein immunoreactive astrocytes in the forebrain parallels stages of intraneuronal pathology in sporadic Parkinson's disease. *Acta Neuropathol.* 114: 231-41. doi:10.1007/s00401-007-0244-3
- [16] Butti C, Santos M, Uppal N, Hof PR (2013) Von Economo neurons: clinical and evolutionary perspectives. *Cortex.* 49: 312-26. doi: 10.1016/j.cortex.2011.10.004
- [17] Christopher L, Koshimori Y, Lang AE, Criaud M, Strafella AP (2014) Uncovering the role of the insula in non-motor symptoms of Parkinson's disease. *Brain* 137: 2143-54. doi: 10.1093/brain/awu084
- [18] Christopher L, Marras C, Duff-Canning S, Koshimori Y, Chen R, Boileau I, Segura B, Monchi O, Lang AE, Rusjan P, Houle S, Strafella AP (2014) Combined insular and striatal dopamine dysfunction are associated with executive deficits in Parkinson's disease with mild cognitive impairment. *Brain* 137: 565-75. doi: 10.1093/brain/awt337
- [19] Craig AD (2009) How do you feel—now? The anterior insula and human awareness. *Nat Rev Neurosci.* 10: 59-70. doi: 10.1038/nrn2555
- [20] Crary JF, Trojanowski JQ, Schneider JA, Abisambra JF, Abner EL, Alafuzoff I, et al. (2014)

- Primary age-related tauopathy (PART): a common pathology associated with human aging. *Acta Neuropathol.* 128: 755-66. doi: 10.1007/s00401-014-1349-0
- [21] Del Tredici K. and Braak H (2016) Review: Sporadic Parkinson's disease: Development and distribution of  $\alpha$ -synuclein pathology. *Neuropathol Appl Neurobiol* 42: 33-50. doi: 10.1111/nan.12298
- [22] Evrard HC, Forro T, Logothetis NK (2012) Von Economo neurons in the anterior insula of the macaque monkey. *Neuron* 74: 482-9. doi: 10.1016/j.neuron.2012.03.003
- [23] Evrard HC, Logothetis NK, Craig AD (2014) Modular architectonic organization of the insula in the macaque monkey. *J Comp Neurol.* 522: 64-97. doi: 10.1002/cne.23436
- [24] Fahn S. (2003) Description of Parkinson's disease as a clinical syndrome. *Ann N Y Acad Sci.* 991: 1-14.
- [25] Flynn, F (1999) Anatomy of the insula functional and clinical correlates. *Aphasiology* 13: 55-78.
- [26] Gallay DS, Gallay MN, Jeanmonod D, Rouiller EM, Morel A (2012) The insula of Reil revisited: multiarchitectonic organization in macaque monkeys. *Cereb Cortex.* 22: 175-90. doi: 10.1093/cercor/bhr104
- [27] Goedert M, Spillantini MG, Del Tredici K, Braak H (2013) 100 years of Lewy pathology. *Nat Rev Neurol* 9: 13-24. doi: 10.1038/nrneurol.2012.242
- [28] Goodkind M, Eickhoff SB, Oathes DJ, Jiang Y, Chang A, Jones-Hagata LB, et al (2015) Identification of a common neurobiological substrate for mental illness. *JAMA Psychiatry.* 72: 305-15. doi: 10.1001/jamapsychiatry.2014.2206
- [29] Hyman BT, Trojanowski JQ (1997) Consensus recommendations for the postmortem diagnosis of Alzheimer disease from the National Institute on Aging and the Reagan Institute Working Group on diagnostic criteria for the neuropathological assessment of Alzheimer disease. *J Neuropathol Exp Neurol.* 56: 1095-7.
- [30] Kalia LV, Lang AE (2015) Parkinson's disease. *The Lancet* 386: 896-912. doi: 10.1016/S0140-6736(14)61393-3
- [31] Kovacs GG, Ferrer I, Grinberg LT, Alafuzoff I, et al. (2016) Aging-related tau astrogliopathy (ARTAG): harmonized evaluation strategy. *Acta Neuropathol.* 131: 87-102. doi: 10.1007/s00401-015-1509-x
- [32] Kurth F, Eickhoff SB, Schleicher A, Hoemke L, Zilles K, Amunts K (2010) Cytoarchitecture and probabilistic maps of the human posterior insular cortex. *Cereb Cortex.* 20: 1448-61. doi: 10.1093/cercor/bhp208
- [33] Lee JE, Cho KH, Song SK, Kim HJ, Lee HS, Sohn YH, Lee PH (2014) Exploratory analysis of neuropsychological and neuroanatomical correlates of progressive mild cognitive impairment in Parkinson's disease. *J Neurol Neurosurg Psychiatry.* 85: 7-16. doi: 10.1136/jnnp-2013-305062
- [34] Mak E, Zhou J, Tan LC, Au WL, Sitoh YY, Kandiah N (2014) Cognitive deficits in mild Parkinson's disease are associated with distinct areas of grey matter atrophy. *J Neurol Neurosurg Psychiatry* 85: 576-80. doi: 10.1136/jnnp-2013-305805
- [35] McKeith I, Mintzer J, Aarsland D, Burn D, Chiu H, Cohen-Mansfield J, et al (2004) Dementia with Lewy bodies. *Lancet Neurol.* 3: 19-28.
- [36] McKeith IG, Dickson DW, Lowe J, Emre M, O'Brien JT et al (2005) Diagnosis and

- management of dementia with Lewy bodies: third report of the DLB Consortium. *Neurology* 65: 1863-72. doi: 10.1212/01.wnl.0000187889.17253.b1
- [37] Mesulam MM, Mufson EJ (1982) Insula of the old world monkey. I. Architectonics in the insulo-orbito-temporal component of the paralimbic brain. *J Comp Neurol.* 212: 1-22.
- [38] Mesulam MM, Mufson EJ (1982) Insula of the old world monkey. III: Efferent cortical output and comments on function. *J Comp Neurol.* 212: 38-52. doi: 10.1002/cne.902120104
- [39] Montine TJ, Phelps CH, Beach TG, Bigio EH, Cairns NJ, Dickson DW, et al (2012) National Institute on Aging-Alzheimer's Association guidelines for the neuropathologic assessment of Alzheimer's disease: a practical approach. *Acta Neuropathol.* 123: 1-11. doi: 10.1007/s00401-011-0910-3
- [40] Morel A, Gallay MN, Baechler A, Wyss M, Gallay DS (2013) The human insula: Architectonic organization and postmortem MRI registration. *Neuroscience* 236: 117-35. doi: 10.1016/j.neuroscience.2012.12.076
- [41] Mufson EJ, Mesulam MM (1982) Insula of the old world monkey. II: Afferent cortical input and comments on the claustrum. *J Comp Neurol.* 212: 23-37. doi: 10.1002/cne.902120103
- [42] Oberheim NA, Goldman SA, Nedergaard M (2012) Heterogeneity of astrocytic form and function. *Methods Mol Biol.* 814: 23-45. doi: 10.1007/978-1-61779-452-0\_3
- [43] Oberheim NA, Takano T, Han X, He W, Lin JH, Wang F, Xu Q, Wyatt JD, Pilcher W, Ojemann JG, Ransom BR, Goldman SA, Nedergaard M (2009) Uniquely hominid features of adult human astrocytes. *J Neurosci.* 29: 3276-87. doi: 10.1523/JNEUROSCI.4707-08.2009
- [44] Postuma RB, Berg D, Stern M, Poewe W, Olanow CW, Oertel W, Marek K, Litvan I, Lang AE, Halliday G, Goetz CG, Gasser T, Dubois B, Chan P, Bloem BR, Adler CH, Deuschl G (2016) Abolishing the 1-year rule: How much evidence will be enough? *Mov Disord.* 31: 1623-1627. doi: 10.1002/mds.26796
- [45] Postuma RB, Berg D, Stern M, Poewe W, Olanow CW, Oertel W, Obeso J, Marek K, Litvan I, Lang AE, Halliday G, Goetz CG, Gasser T, Dubois B, Chan P, Bloem BR, Adler CH, Deuschl G (2015) MDS clinical diagnostic criteria for Parkinson's disease. *Mov Disord.* 30: 1591-601. doi: 10.1002/mds.26424
- [46] Seeley WW, Carlin DA, Allman JM, Macedo MN, Bush C, Miller BL, Dearmond SJ (2006) Early frontotemporal dementia targets neurons unique to apes and humans. *Ann Neurol.* 60: 660-7. doi: 10.1002/ana.21055
- [47] Seeley WW, Merkle FT, Gaus SE, Craig AD, Allman JM, Hof PR (2012) Distinctive neurons of the anterior cingulate and frontoinsula cortex: a historical perspective. *Cereb Cortex.* 22: 245-50 . doi: 10.1093/cercor/bhr005
- [48] Sengupta U, Guerrero-Muñoz MJ, Castillo-Carranza DL, Lasagna-Reeves CA, Gerson JE, Paulucci-Holthauzen AA, et al (2015) Pathological interface between oligomeric alpha-synuclein and tau in synucleinopathies. *Biol Psychiatry.* 78: 672-83. doi: 10.1016/j.biopsych.2014.12.019
- [49] Stevens, C. and Halliday, G (2014) The Role of Astrocytes in Parkinson's Disease. In: *Inflammation in Parkinson's Disease: Scientific and Clinical Aspects.* Springer, Switzerland, pp 127-144 .

- [50] Svenningsson P, Westman E, Ballard C, Aarsland D (2012) Cognitive impairment in patients with Parkinson's disease: diagnosis, biomarkers, and treatment. *Lancet Neurol.* 11: 697-707. doi: 10.1016/S1474-4422(12)70152-7
- [51] Thal DR, Rüb U, Orantes M, Braak H (2002) Phases of A beta-deposition in the human brain and its relevance for the development of AD. *Neurology.* 58: 1791-800.
- [52] Yarnall A, Rochester L, Burn DJ (2011) The interplay of cholinergic function, attention, and falls in Parkinson's disease. *Mov Disord.* 26: 2496-503. doi: 10.1002/mds.23932

# Tables

**Table 1 Subject demographics and neuropathological staging**

#	HC-1	HC-2	iLBD-1	PD-1	PD-2	PDD-1	PDD-2	PDD-3	DLB-1	DLB-2
Sex	F	M	F	M	F	M	F	M	M	M
Clinical Diagnosis	HC	HC	HC	PD	PD	PDD	PDD	PDD	DLB	DLB
Age at death (yr)	78	70	88	78	93	74	88	81	67	75
Pathological diagnosis	Control	Control	iLBD	PD	PD	PDD	PDD	PDD	DLB	DLB
Age of onset	-	-	-	75	91	67	73	77	62	73
Disease Duration	-	-	-	3	2	7	15	4	5	2
Braak $\alpha$ -syn	-	-	4	3	3	6	5	6	6	6
Braak NFT & tauopathy	-	-	3	1	2	2 + ARTAG	2 + ARTAG, PART	3	5	3
Thal phase B-amyloid	-	-	2	0	2	3	0	3	5	4
ABC score	-	-	A3B2C1	A0B1C0	A1B1C0	A2B1C0	A0B1C0	A2B2C0	A3B3C3	A2B2C3
Psychiatric symptoms	-	-	-	-	Depression	Delirium, Anxiety, RBD, Hallucinations	Depression, Panic attacks, Hallucinations	RBD, Anxiety, Depression, Disinhibition, Hallucinations	RBD, Hallucinations, Apraxia, Capgras syndrome	Paranoia, Psychosis, Hallucinations

Table 1 Subject Demographics and neuropathological staging. ABC score: A-C(0-3), ARTAG: Aging-related tau astroglialopathy, Braak NFT:0-6, Braak  $\alpha$ -syn: 0-6 DLB: Dementia with Lewy bodies, HC: Healthy control, iLBD: incidental Lewy body disease, LBV: Lewy body variant, NFT: neurofibrillary tangles, PART: primary age-related tauopathy, PD: parkinson's disease, RBD: REM sleep behavioral disorder, Thal phase: 0-5,  $\alpha$ -syn:  $\alpha$ -synuclein,-: none/absent

# 1.1 Figure 1

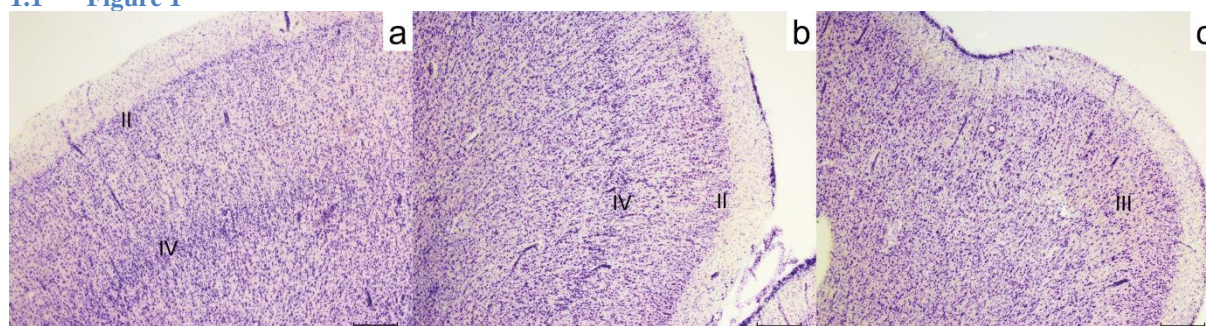


**Fig. 1 Definition of Insular sub-regions in 60  $\mu$ m thick sections.** (a) Granular insular grey matter shows uniform and well defined granular layers II and IV in an iLBD case. (b) Dysgranular insula shows less dense and granular layers II and IV. (c) Agranular insula grey matter is shown lacking layers II and IV. iLBD: incidental Lewy body disease, II: layer two, III: layer three, IV: layer four. Magnification: 25x, scale bar 500  $\mu$ m

**Figure 2**

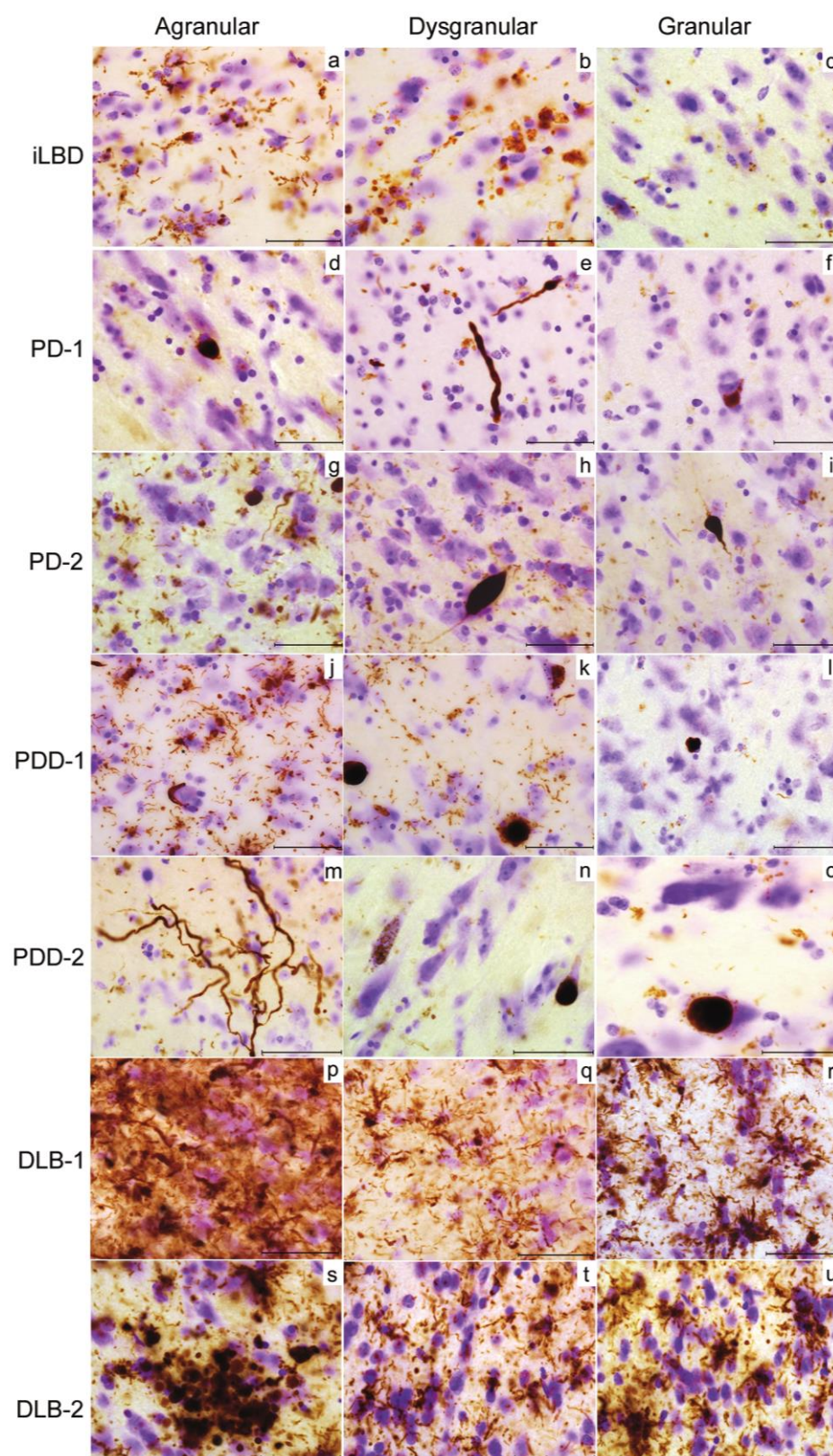


**Fig. 2 Distribution pattern of  $\alpha$ -synuclein in insular sub-regions.** iLBD shows mild LNs and astroglial  $\alpha$ -synuclein inclusions in layer I of agranular insula (**a**), few glial inclusions in dysgranular insula (**b**), and sparse dot-like aggregates in granular insula (**c**). PD-1 agranular insula shows a LB-like inclusion and dot-like

aggregates (**d**), the dysgranular insula shows bulgy LNs in layer I (**e**), and the granular insula shows an intracellular LB inclusion (**f**). PD-2 shows many LNs inclusions in agranular insula and glial  $\alpha$ -synuclein (**g**) and less but bulgy LN in dysgranular (**h**) and granular regions (**i**). In PDD-2 severe astroglial  $\alpha$ -synuclein inclusions are shown in agranular insula (**j**) few LBs and LNs in dysgranular insula (**k**). The granular insula shows dot-like aggregates and astroglial  $\alpha$ -synuclein (**l**). In PDD-1 agranular insula, very long LNs and some dot-like aggregates are seen in layer I (**m**). Dysgranular insula in PDD-1 shows granular cytoplasmic inclusions in neurons and a LB (**n**) while the granular insula shows less aggregates and a LB in the infragranular layer (**o**). In DLB-1, severe  $\alpha$ -synuclein inclusions are seen in agranular insula throughout all layers (**p**). Severe astroglial inclusions are seen in the supragranular layers of dysgranular and granular insula (**q-r**). In DLB-2, a cluster of dystrophic LNs and glial inclusions are shown in layer II of the agranular insula (**s**). The dysgranular insula contains LNs and dot-like structures (**t**) also abundant in the granular insula superficial layers (**u**). DLB: dementia with Lewy bodies, iLBD: incidental Lewy body disease, LB: Lewy bodies, LN: Lewy neurites, PD: Parkinson's disease, PDD: parkinson's disease dementia. Magnification: 630x, scale bar 50 $\mu$ m

**Figure 3**

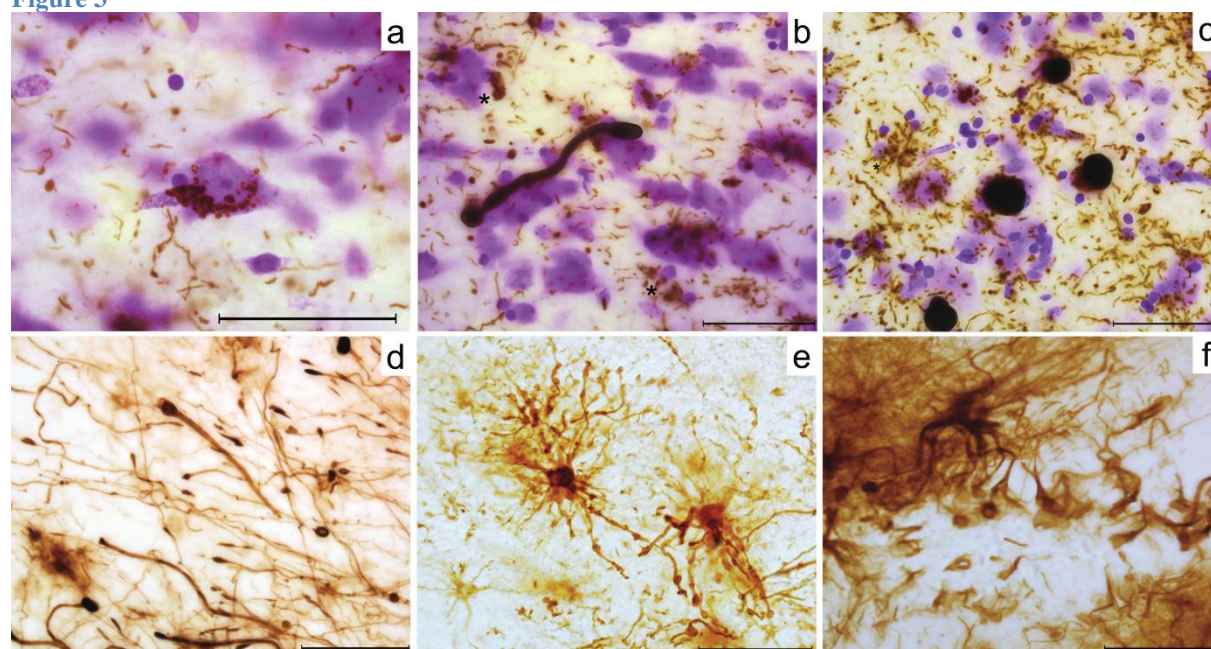


**Fig. 3 Cell specific morphology and inclusions in Lewy body diseases.** In PDD-2 with astroglial tauopathy, infragranular layer of agranular insula show astroglial-to-neuronal  $\alpha$ -synuclein inclusions (**a**), an elongated  $\alpha$ -synuclein positive process with bulbous endings (possibly glial) surrounded by astroglial  $\alpha$ -synuclein inclusions (\*) and LNs (**b**). DLB-2 shows LB inclusions, LNs, and astroglial  $\alpha$ -synuclein (\*) within the deep infragranular layer (**c**). Loose GFAP +ve astrocytic processes are shown containing bulbous end feet and donut-shaped structures in the supragranular layers of the agranular insula in DLB-2 (**d**). PDD-1 with astroglial tauopathy shows small and dysmorphic astrocytes containing multiple varicosities within their processes, possibly fuzzy astrocytes (**e**). A GFAP +ve astrocyte is shown surrounded by unorganized processes in DLB-2 (**f**). Magnification: 630x, scale bar 50 $\mu$ m

**Figure 4**

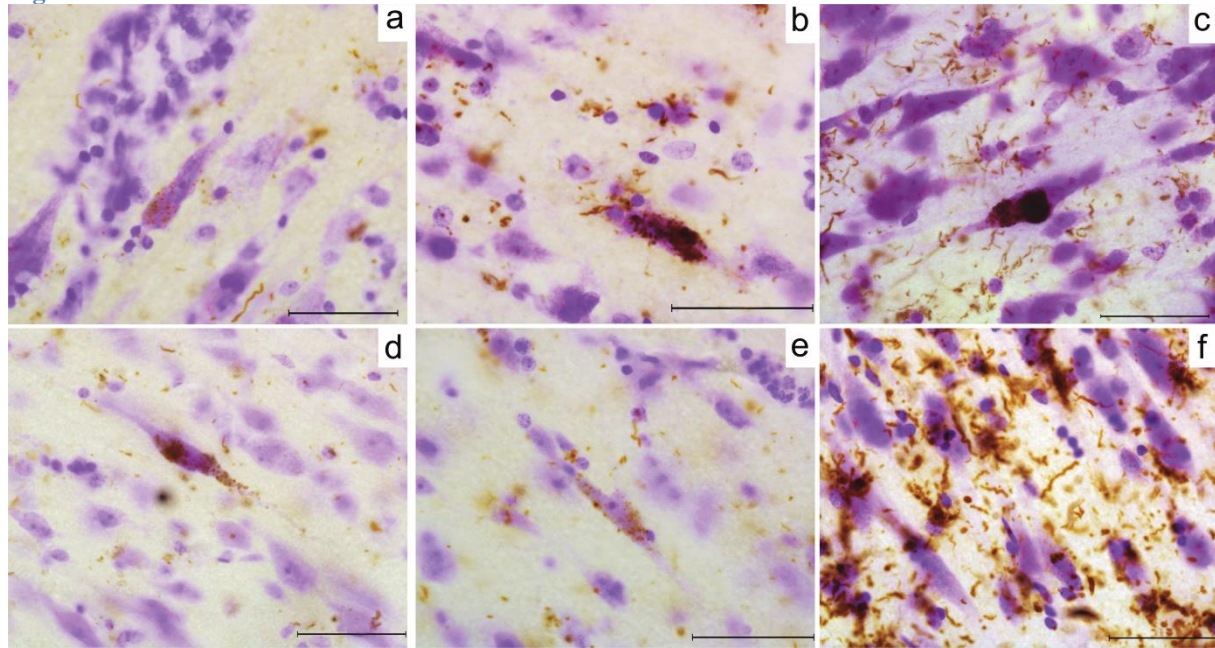


**Fig. 4  $\alpha$ -synuclein deposits in VEN and fork cell.** (a) PD-2 shows granular LB inclusions (brown) along a VEN. (b) LB in VEN and surrounding astrocytes in PD-2. (c) PDD-2 shows a VEN containing a large LB and multiple granular inclusions within the cell body, astroglial  $\alpha$ -synuclein inclusions are also seen. (d) PDD-1 shows LB in the soma and dendrite of a VEN. (e)  $\alpha$ -synuclein inclusions are shown in a fork cell in PDD-1. (f) DLB-2 agranular region shows many deposits surrounding and inflicting pyramidal neurons and rod shaped VEN. Magnification: 630x, scale bar 50 $\mu$ m

**Figure 5**

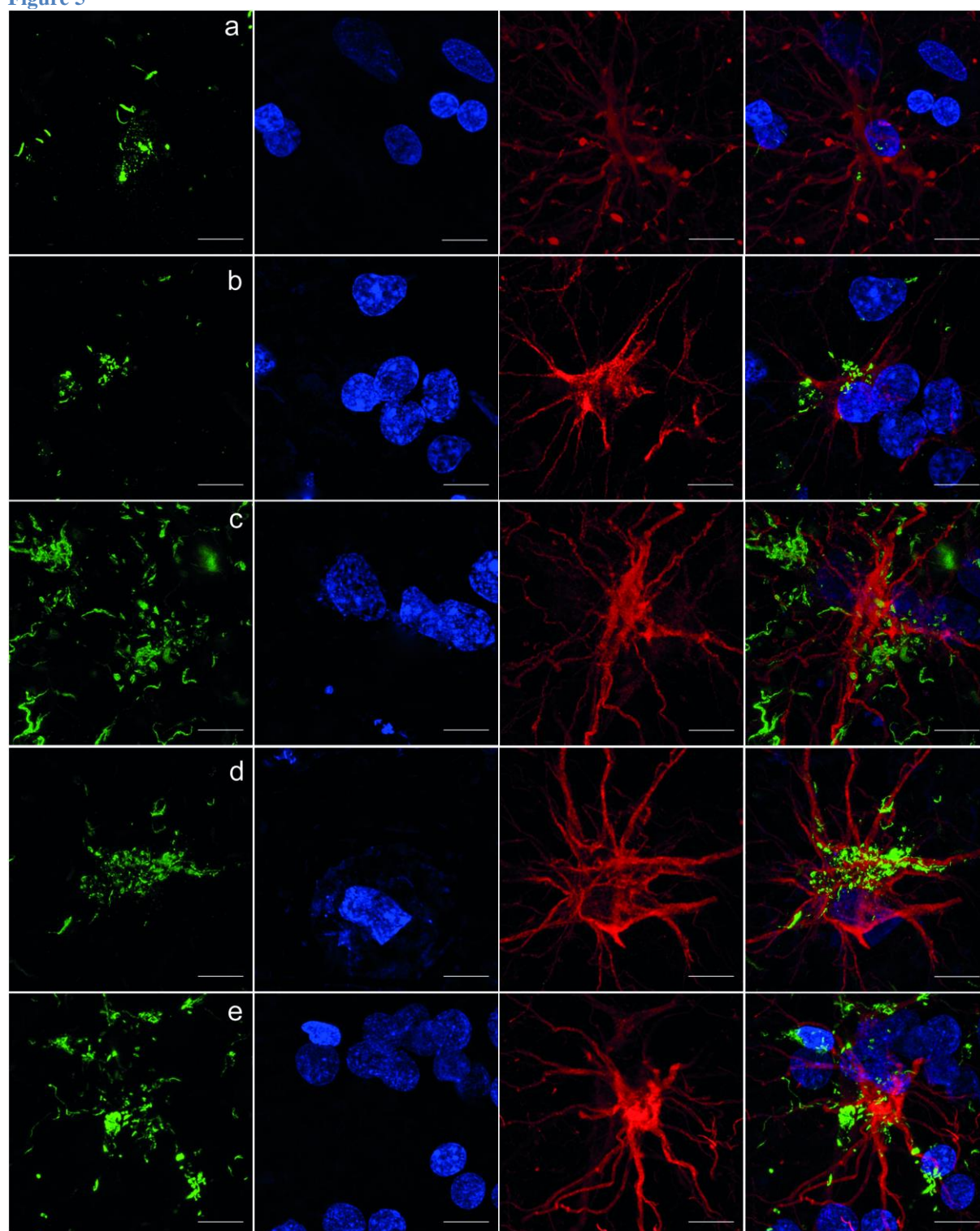


**Fig. 5 Relationship between  $\alpha$ -synuclein immunoreactivity and astrocytes in insular cortex in PD(D) and DLB.**  $\alpha$ -synuclein (green) is present within varicose projection astrocyte (GFAP, red) cell body in infragranular layer, anterior insula in PD-2 (a). In PDD-2, an astrocyte is shown containing  $\alpha$ -synuclein aggregates and surrounded by a cluster of nuclei, probably neuronal, in the anterior insula (b). And in PDD-3, a protoplasmic astrocyte is shown surrounded by multiple  $\alpha$ -synuclein aggregates (c). DLB-1 shows  $\alpha$ -synuclein deposits surrounding the cell body of an interlaminar astrocyte in layer I (d) and similar inclusions are shown within a protoplasmic astrocyte, its processes, and the surrounding clustered nuclei in posterior insula (e). Magnification 100x. Scale bar: 10 $\mu$ m